Design and Lessons Learned on the Development of a Cryogenic Pupil Select Mechanism used in the Testing and Calibration of the Integrated Science Instrument Module (ISIM) on the James Webb Space Telescope (JWST)

Alissa Mitchell*, Thomas Capon*, Jeffrey Guzek**, Claef Hakun*, Paul Haney* and Corina Koca*

Abstract

Calibration and testing of the instruments on the Integrated Science Instrument Module (ISIM) of the James Webb Space Telescope (JWST) is being performed by the use of a cryogenic, full-field, optical simulator that was constructed for this purpose. The Pupil Select Mechanism (PSM) assembly is one of several mechanisms and optical elements that compose the Optical Telescope Element SIMulator, or OSIM. The PSM allows for several optical elements to be inserted into the optical plane of OSIM, introducing a variety of aberrations, distortions, obscurations, and other calibration states into the pupil plane. The following discussion focuses on the details of the design evolution, analysis, build, and test of this mechanism along with the challenges associated with creating a sub arc-minute positioning mechanism operating in an extreme cryogenic environment. In addition, difficult challenges in the control system design will be discussed including the incorporation of closed-loop feedback control into a system that was designed to operate in an open-loop fashion.

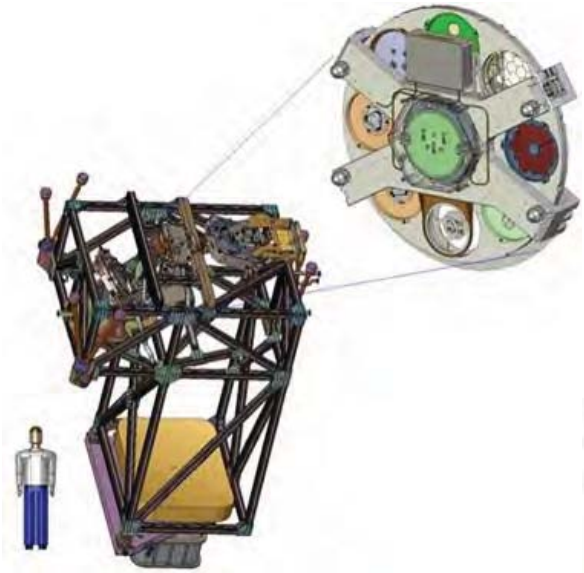

Figure 1. PSM in OSIM Bench

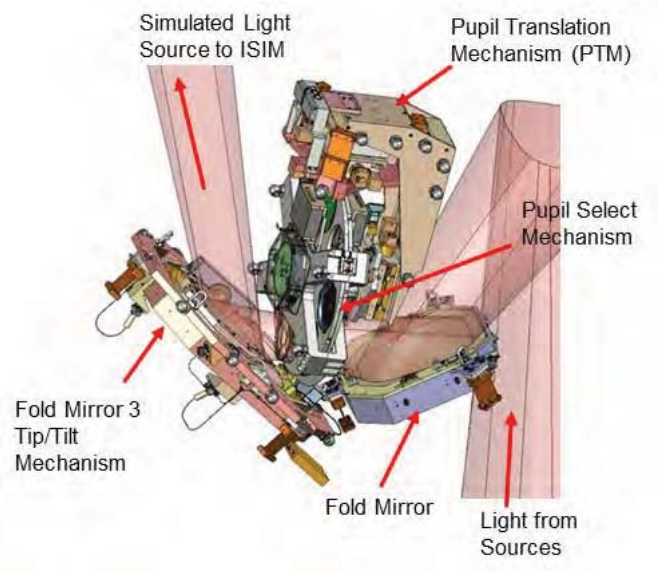

Figure 2. Light Path through PSM

Introduction

The JWST Optical Simulator (OSIM) is designed to simulate the optical performance of the JWST telescope elements. The simulator consists of the primary imaging optical path, which relays fiber optic point sources to the focal surface of the ISIM over its field of view. OSIM is comprised of several subassemblies, including the Optical Bench Module (OBM), into which the PSM is integrated. The PSM is located at the pupil plane of the OSIM instrument and is mounted on a 2-DOF Pupil Translation

* NASA Goddard Space Flight Center, Greenbelt, MD

** Design Interface, Inc. Greenbelt, MD

Mechanism. Figures 1 and 2 show the location of the PSM within the OSIM optical bench. For a more detailed description of the OSIM, see reference 2.

Integration of the various modules and subassemblies into OSIM occurred at GSFC in the Spacecraft Systems Development and Integration Facility (SSDIF) and environmental performance of OSIM was verified in the Space Environment Simulator (SES), where OSIM was tested with the Beam Image Analyzer (BIA). The BIA is a cryogenic 5 DOF mechanism system with cold focal planes designed by NASA/GSFC Electromechanical Systems Branch and was used to measure the performance of OSIM as the simulator for the JWST optical telescope. Figure 3 shows the OSIM being lowered in to the SES chamber. Figure 4 shows the OSIM during ambient alignment with the BIA in the SSDIF.

Figure 3. OSIM Bench being lowered into the SES

Figure 4. OSIM during Ambient Alignment

The PSM provides OSIM with the capability to configure the OSIM pupil plane with various optical elements, masks, and alignment reference sources. In this mechanism, two 27-inch (68.6-cm) wheel assemblies are assembled adjacent to one another with 0.1 inch (2.5 mm) of clearance between them. Fourteen different optical elements, eight in each wheel, are then rotated into the optical plane of OSIM for testing and calibration purposes. Driving requirements for the PSM are to operate in a cryogenic environment and to provide stable and repeatable positioning of the elements in the optical plane during a powered-off condition. During the testing stages of OSIM, the PSM is required to operate at temperatures as low as 100K and with element position placement of less than 45 arc-seconds. A brief description of the elements located in the two wheels is shown in Figure 5.

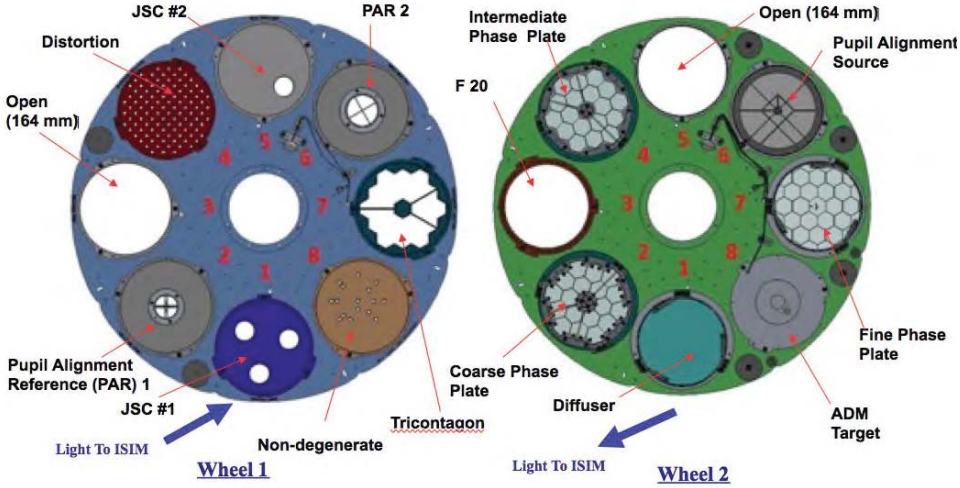

Figure 5. PSM Wheel Optical Elements

All of the elements in Wheel 1 were fabricated from 6061 Aluminum and machined to tolerances to meet the requirements of each individual element. It should be noted that, in addition to mounting the optical

elements, heaters and temperature sensors were also mounted on each wheel. In addition, the ADM Target incorporated an LED light source. These necessitated the incorporation of a cable wrap into both wheel assemblies. The optical elements in wheel 2 were more complex, precision opto-mechanical assemblies. An example is the Course Phase Plate Assembly. Figure 6 shows the course phase plate which incorporated sophisticated fabrication and assembly techniques to allow for the individual mounting of 18 segments that would not distort when cooled from ambient temperature to 100 Kelvin.

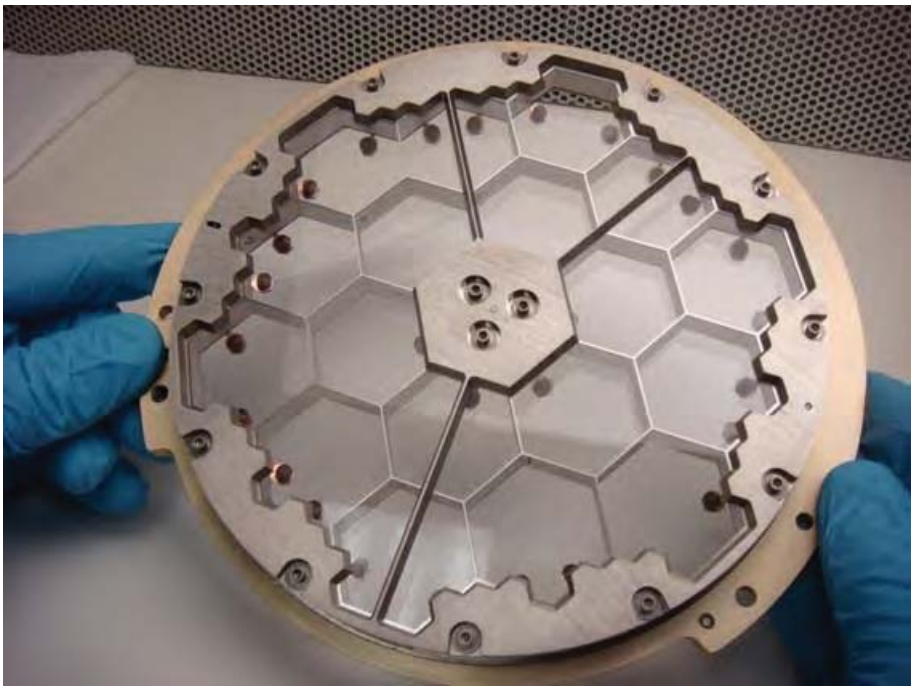

Figure 6. PSM Optical Element Phase Plate

Design Evolution of the PSM

During the conceptual design phase of the PSM, the most challenging design task was to develop a system with high pointing stability and repeatability in the powered-off state. Two spare CDA gearhead stepper motors that had been used on a previous JWST mechanism life test were available for the development. This motor was incorporated into the design to turn the primary wheel via friction from a preloaded drive wheel. The step size of the stepper motor allowed for a position resolution of less than 45 arc-seconds, while a high accuracy absolute encoder provided knowledge information to a resolution of approximately 1 arc-second. Figure 7 shows the initial conceptual design of the traction drive system.

A peer review was held on the design and significant resources were dedicated to proof-of-concept. During the initial stages, motor testing was performed as well as testing on high friction representative materials for the optical element wheel and the drive wheel. Several materials were considered for the drive wheel including Vespel, a polymer/carbon fiber blend composite (WearComp®), and a polymer/carbon fiber/graphite composite blend (FibreComp®). Tests were performed to capture the friction coefficient between these potential materials and the aluminum wheel and to determine a viable pairing that offered a high coefficient of friction with a low risk of debris generation. These tests were performed in ambient pressure and in vacuum at several temperatures, down to 100K, and displayed an unacceptable amount of variation in the coefficient of friction.

Due to concerns with motor life, power dissipation, the variability of the friction data under cold temperature, and a concern that the motor drive wheel would slip during operation, it was decided that pursuing a different design route for the PSM would be less risky. As the development schedule for the

PSM was constrained, the goal was to limit design modifications to the friction-based PSM and to incorporate the high-accuracy, low-bandwidth sensor from the original concept. In addition, restricted wire counts in the flex harness that provided power and signal to the encoders precluded the addition of a high-rate position sensor to the design.

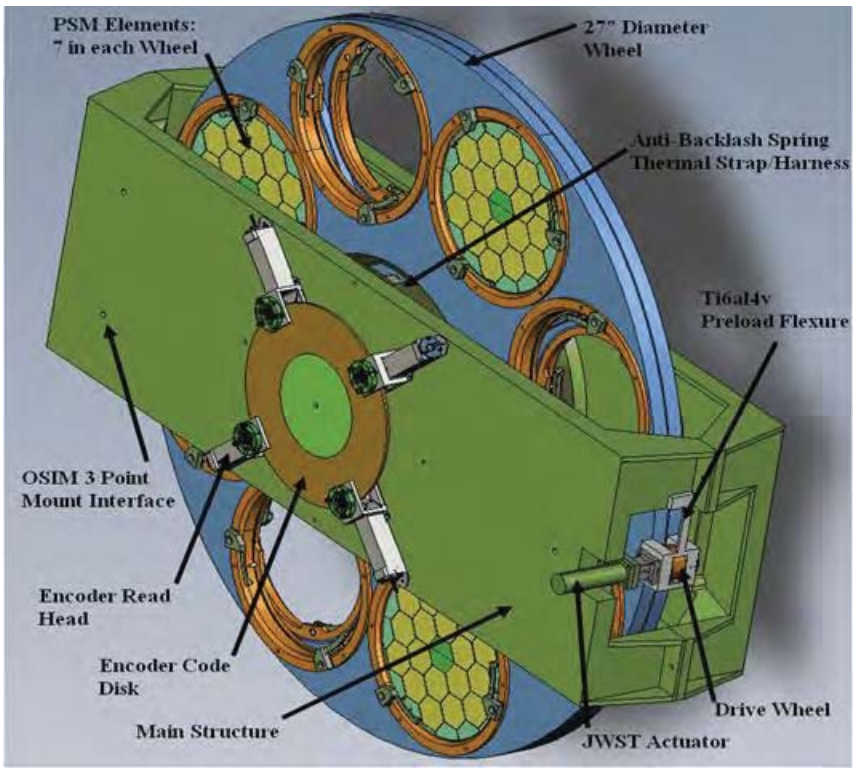

Figure 7. Preliminary PSM Friction Drive Design

The team began a conceptual redesign incorporating a brushless DC motor to directly drive each PSM wheel. At a later time, a preloaded follower wheel was added on the outside of the mechanism that would engage mechanical detents machined into the wheel. In addition to preliminary control system design modeling, analyses were initiated to determine the optimal detent and follower wheel geometries as well as the forces on the system. The initial analysis showed that an open-loop control system could be developed to meet the power-off position requirement with minimal changes to the initial friction-based conceptual design.

As-Built PSM Design

In order to rotate the wheels, the stepper motors were replaced by two frameless, 2-phase brushless Aeroflex motors affixed to the center hub assembly, directly driving each wheel. The hub assembly also includes spring-loaded angular contact bearings. In order to meet the 45 arc-second holding and repeatability positioning requirement, a detent is used on the outside of the wheel with a follower assembly to roll in and out of the detents and to hold the wheel in place when power is removed. The encoder system was developed to operate in the 100K environment and provided feedback for the mechanism electronics. Ultimately, it was determined that in order to control the mechanism, a high-fidelity dynamic model was needed. The dynamics of the system were modeled along with a PID gain scheduling controller and trajectory planning which utilized 40-Hz feedback from the absolute encoder system. The final design of the PSM is shown in Figure 8. Details of the maturation will be discussed below.

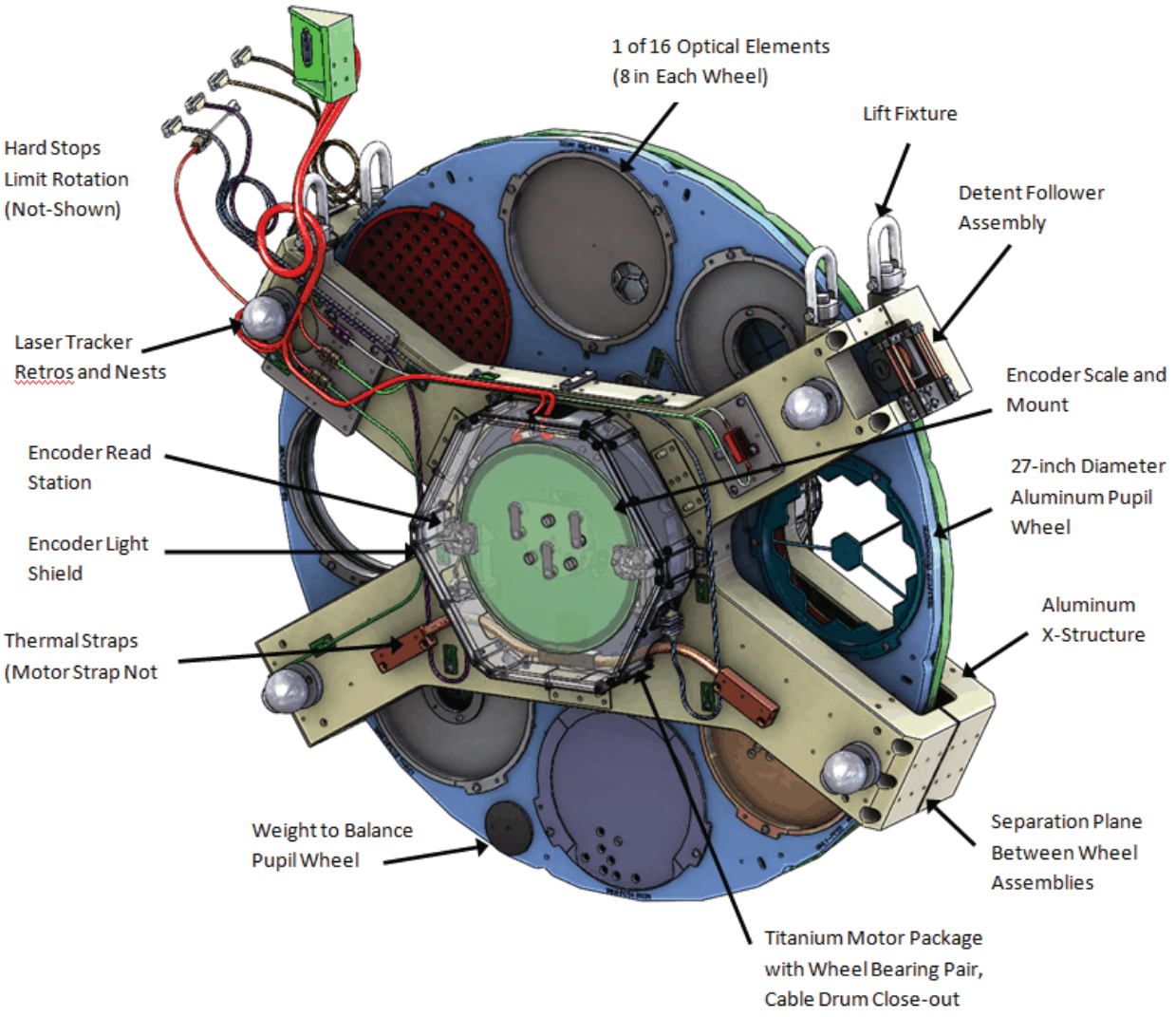

Figure 8. As-Built PSM Design

Motor/ Bearing Hub Assembly

To drive the PSM, two frameless, brushless DC motors were selected from Aeroflex and mounted directly to the frame of the structure. In the sizing of these motors, it was assumed that the primary purpose of the motors was to drive the wheels to the capture region of the follower wheel and, therefore, no control authority was required.

Due to the cryogenic operating temperatures, traditional bearing lubricants were not suitable for the application, and the bearings needed to be cold-treated to the 100K operating temperatures of the mechanism. Ultimately, a hybrid, dry-running ceramic bearing from Cerobear was selected for this application. The bearings consisted of a non-magnetic, silicon nitride balls running in Cronidur 30 races with minimum lubrication from PGM-HT (PTFE/MoS_2/glass fibre composite) retainers. The hardness properties of the ceramic balls coupled with the material differences between the balls and the steel races reduces the risk of fretting, cold welding, and seizing of the bearing at higher Hertzian stresses. The expected of number life cycles for the mechanism was 2000, which is an acceptable lifetime to expect for these bearings. To accommodate the large operating temperature range, the PSM bearings were installed with a soft preload, such that the maximum loaded bearing had a mean Hertzian pressure of

101 ksi (696 MPa), which is less than half the mean recommended Hertzian pressure of 217 ksi (1496 MPa) from the vendor. A cross-section of the wheel assemblies is shown in Figure 9.

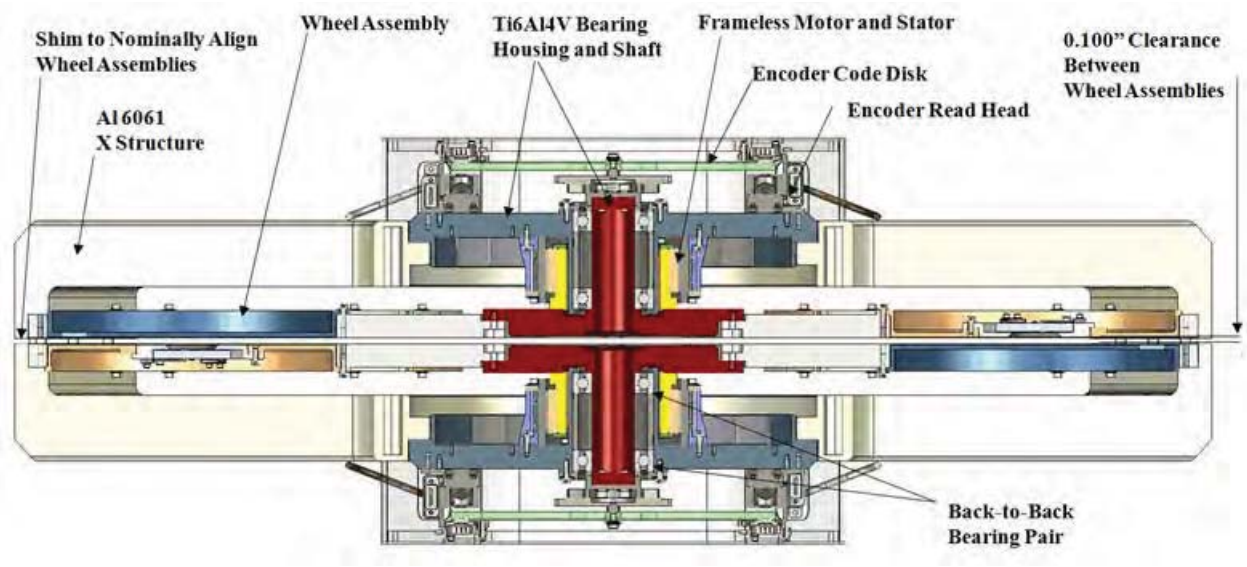

Figure 9. Cross-section of Wheel Assemblies

The motors and motor bearings were assembled together in a titanium hub which provided a good coefficient of thermal expansion (CTE) match to the bearing race material. Figure 10 shows the fixture used to assemble the motor rotor and stator. To accommodate CTE mismatch between the titanium hub and the aluminum wheels and X-frame structure, three pin-in-slot interfaces coupled with controlled fastener preload were used to accommodate sliding during cool-down. For signals transversing the rotating axis, a flat ribbon cable from 3M was used in a coiled clock spring design to allow for near 360° rotation. Prior to assembly, this ribbon cable was heated on a mandrel to create a coiled shape, which assisted in assembly. Figure 11 shows the cable wrap assembly.

Figure 10. Motor Rotor Manually Lowered into Stator Assembly

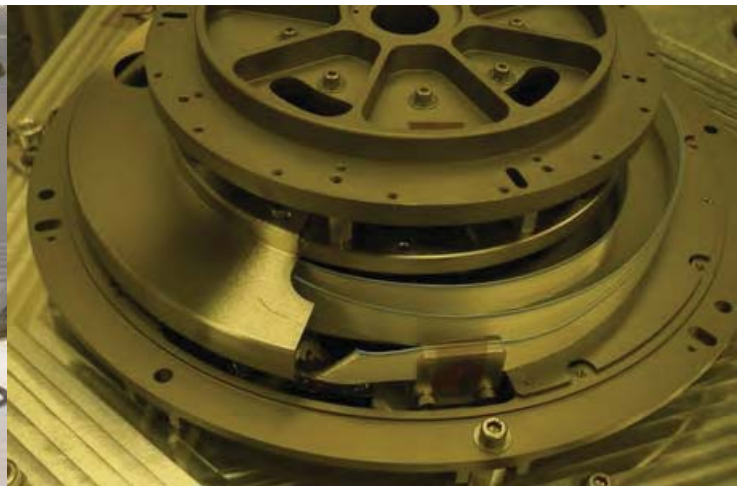

Figure 11. Cable Wrap Assembly

Follower Wheel Assembly

For the follower wheel, Vespel (SP-1) was selected due to the low risk of debris generation with the aluminum wheel. WearComp was also considered for the follower wheel material, but there were concerns that the machined surface finish would generate debris when in contact with the primary wheel. The follower wheel assembly consisted of a face-to-face, spring-loaded duplex bearing pair that supported the follower wheel. The follower wheel was keyed to the rotating shaft while a titanium housing supported the outer races of the bearings. Figure 12 shows the components of the follower wheel assembly.

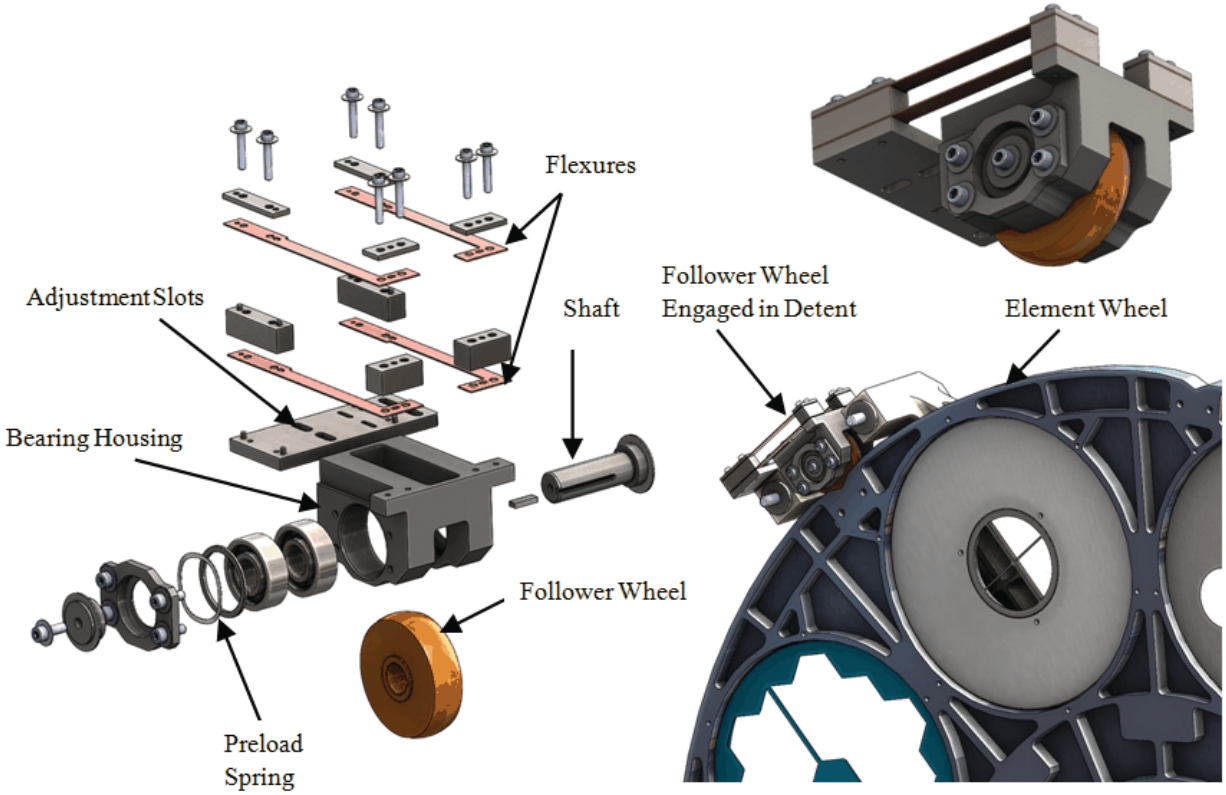

Figure 12. Follower Wheel Assembly

The follower wheel was preloaded on the rim of the element wheel via beryllium copper beam flexures. Slots in the flexure bolt holes allowed for circumferential adjustability of the follower assembly on the x-structure while shims allowed for adjustment of the preload.

The initial design of the follower wheel assembly consisted of two cantilever beams which radially preloaded the follower against the outside surface of the wheel and mechanical detents. Once the assembly was integrated, it became apparent that the cantilever beam preload system had a few shortcomings. The cantilever beam spring allowed for the follower to move in and out of the detent, but did not react moments. The arc-shaped tip motion did not adequately provide a purely radial preload to the follower wheel and did not position the elements in the proper location. The system was replaced with a parallel blade arrangement which allows for near perfect radial motion of the follower as it moves in and out of the mechanical detents while resisting internal moments. This allowed for the optical elements to be positioned as originally envisioned. Figure 13 shows the follower wheel assembly integrated onto the X-frame structure of the PSM.

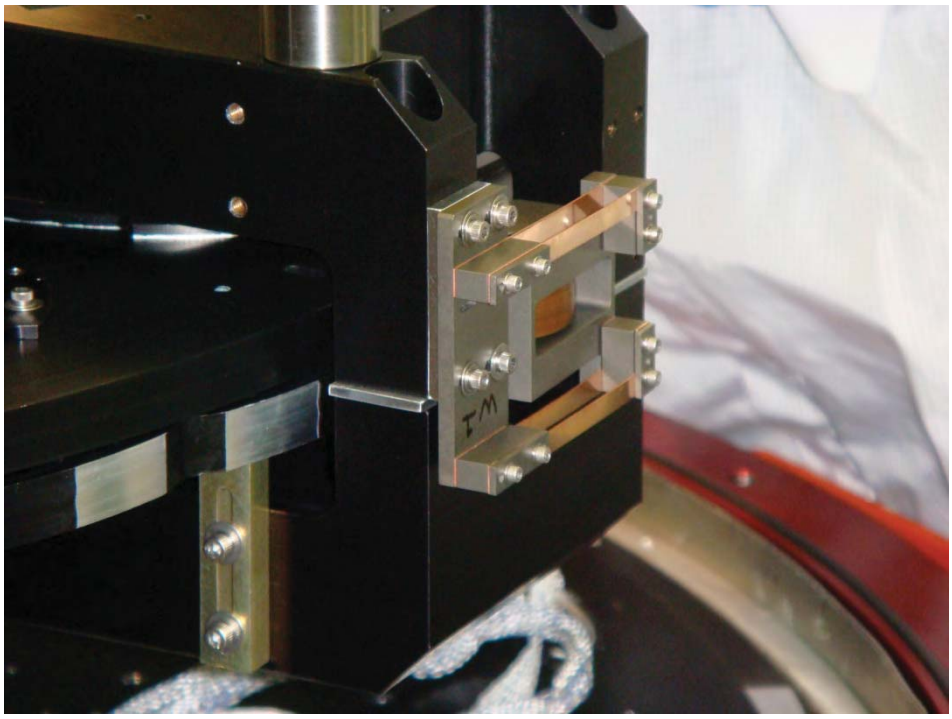

Figure 11. As-Built Mechanical Follower Wheel Assembly

Optical Encoder Design and Development

In order to verify the tight positioning and knowledge requirements, cryogenic absolute encoders were developed (see Reference 1 for more details). The PSM absolute encoders were able to achieve less than one arc-second resolution over a nearly 360-degree operational range. The ultra-high resolution was achieved through a unique process of pattern recognition. A PSM Leviton absolute encoder is shown in Figures 14 and 15, and is composed of an LED and LED pinhole mount, a titanium encoder housing with an internal baffle, a mirror and flexure, a detachable titanium CCD mount with accompanying CCD camera and heater and a photolithographic soda lime glass scale. The rotary scale disc was comprised of a pattern containing a periodic series of lines; each line is etched with unique and identifiable features.

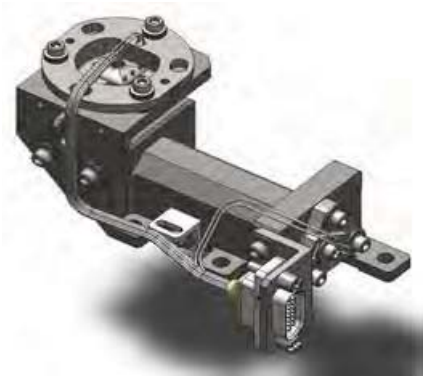

Figure 14. PSM Encoder Readhead

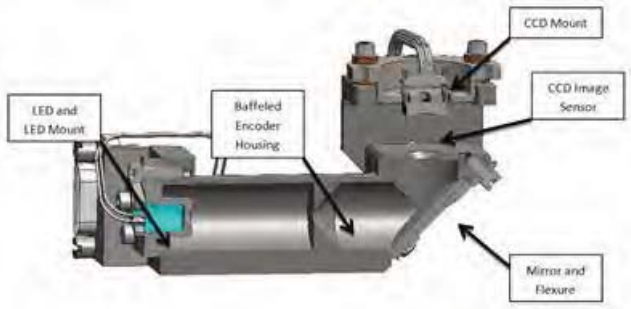

Figure 15. PSM Encoder Cross Section

The encoder functions in the following manner. The LED source emits light and the pinhole collimates the light source to a point source. The light then enters the housing, which is baffled to eliminate undesirable stray light. Once the light exits the housing the scale casts a shadow and the image sensor captures the

unique pattern at that location. In addition to capturing the pattern, the image sensor compares its fixed pixel columns with the centroid of each line on the scale. With the combination of unique and identifiable line features and relative line centroid locations, an absolute position measurement with arcsecond resolution is achieved. Figure 16 and 17 show the assembled read head and the code disk kinematically mounted on the wheel hub assembly.

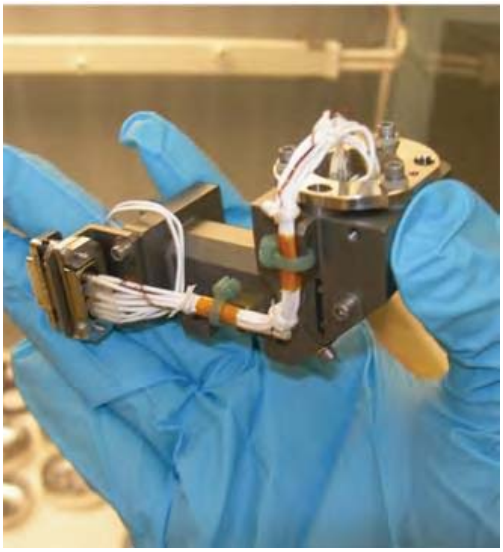

Figure 16. PSM Encoder Readhead

Figure 17. PSM Encoder Disk

Optical Encoder Alignment

Due to the high accuracy requirement of the PSM encoders, alignment was critical; this includes initial alignment as well as alignment repeatability. Omitting the translation of the object being measured, if the encoder read head and scale move relative to each other, the position measurement is void. Two readheads were included to increase accuracy by removing run-out of the bearing configuration. A challenge when operating in a cryogenic environment is designing and accounting for the differing CTEs of the various materials. To control the position of the CCD relative to its mount, a bonding fixture was used. With the CCD position controlled, bonded and fixed in place on the CCD mount, any additional alignment adjustments were made with the CCD mount, specifically minimal decenter, angular position and image sensor to scale defocus adjustments. To maintain alignment, the CCD mount was pinned to the encoder housing and the encoder housing was pinned to the stationary PSM reference.

To ensure the PSM scale was aligned to the rotor and stator over the temperature range, the scale utilized a titanium 3-point kinematic mount with a flat, a cone, and v-groove features. Titanium flexures and features machined into the glass allowed captured steel balls to remain nestled and preloaded between the glass and the mount. In this configuration, all changes in motion of the scale due to thermal contraction and/or expansion were relative to the kinematic mount cone feature. However, due to CTE differences between the glass scale and the titanium hub of the PSM, scale recalibration at varying operational temperatures was performed as part of the PSM testing. In addition, changes to the bias voltage of the CCD were required to allow for good encoder images to be obtained.

PSM Controller Design and Development

Due to the tight requirements and the torque disturbances from the mechanical detent, controlling the Pupil Select Mechanism proved to be much more challenging than originally anticipated. After the baseline of the friction wheel design with geared stepper motor drives was abandoned, and the direct-drive brushless system was implemented, representative testing was performed with an unpopulated

PSM wheel. This initial testing was promising as the control system was able to command the wheel position using the high-accuracy, low-bandwidth encoders. However, when inertial simulators for the optical elements were installed, an open-loop control was not possible with the torque available from the direct drive motors. Therefore, a closed-loop system was developed within the pre-existing design constraints.

The only sensor on the wheels was the high-precision CCD encoder. The readout software was modified to transmit encoder readings to the motor control rack using UDP packets as TCP packets were not delivered fast enough. There was still some variability, so timestamps were added to each measurement and the controller was designed to account for this in speed calculations. In its normal configuration, this encoder only produced 10 measurements per second, and could not produce readings at all above a certain wheel velocity because of image blurring.

Such low sensor bandwidth meant that the optical positioning requirements could not be met through continuous closed-loop control, so mechanical spring-loaded detents were added to the wheel for this purpose. Thus, in addition to a relatively low amount of motor torque for the given inertia, the control system had to deal with the detent as a torque disturbance. As the roller navigated the sharp V-notch in the wheel, it produced very large torques during entry and exit. It seemed impossible to control wheel-exit trajectories, since the low bandwidth and high disturbance produced high exit velocities, and the resulting blurred images disabled feedback control during recovery. Two critical modifications were made to the system to correct this problem. First, the sharp V-notch was replaced with a rounded notch, making the torque disturbance more gradual (see Figure 18). Second, the encoder readout system was modified to use a shorter exposure time, increasing both the measurement rate and the blurring speed limit. The new detent profile reduced the exit speed to well below the new blurring speed limit. Together, these modifications made the system controllable using a gain-scheduled PID controller.

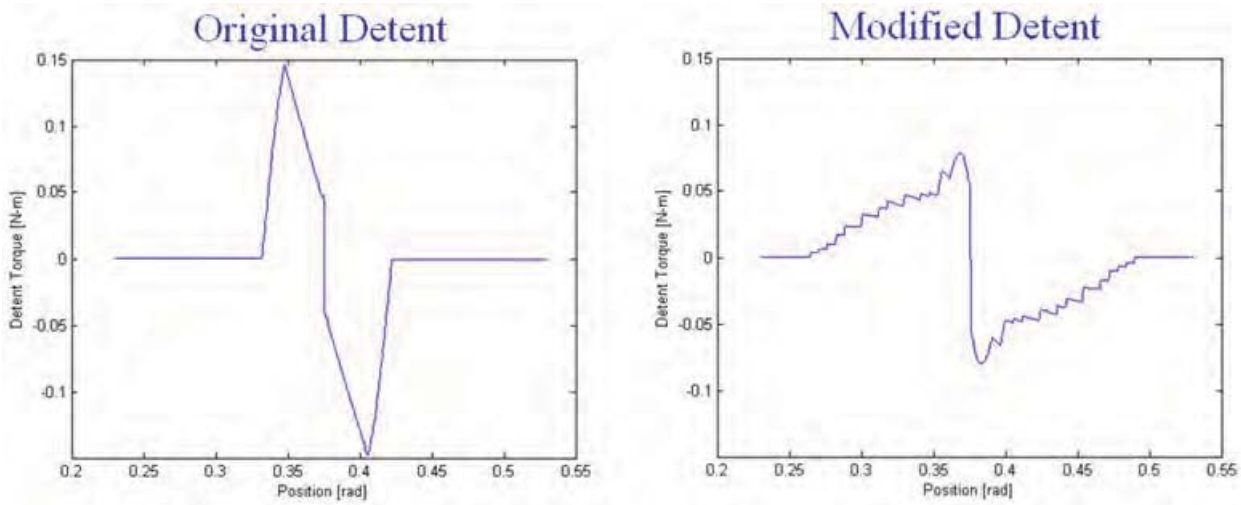

Figure 18. Simulated Detent Disturbance Torque Profile Before and After Mechanical Modification

The gain-scheduled PID controller was developed first in a Simulink model of the wheel, motor, detent, and encoder. While it was very helpful in developing the concept of the controller, the simulation proved too unfaithful for the controller to be directly ported to the physical system. Instead, a similar controller was developed in LabVIEW and the gains tuned during testing. The final version of the controller includes four states that are executed to move from one detent to the next (see Figure 19). Longer moves are composed by repeating single moves, since passing through a detent at speed imparts unpredictable and harmful mechanical shocks to the wheels and optical elements. In all the closed-loop states, the motor is commutated in software based on the encoder readings. The states are as follows:

1. **Exit detent.** A simple integrator is used to ramp up the torque until the wheel leaves the detent. This step is effectively open-loop, because the feedback system is too slow to react to the detent torques. Closed-loop control cannot be used while in the “region of influence” of the detent.
2. **Null velocity.** Once the wheel exits the detent, true closed-loop control can begin. A damping controller brings the wheel to a controller stop just outside the detent, so the remaining states are not affected by variations in exit velocity. These variations are clearly visible in circle 2 of Figure 14.
3. **Trajectory travel.** A linear trajectory with acceleration and deceleration curves is generated to guide the wheel from its present location to the edge of the next detent. A carefully tuned PID controller follows this trajectory and ensures the velocity is close to zero when the detent is reached.
4. **Enter detent.** The closed-loop controller is disabled just inside the “region of influence” of the detent. Instead, a high-current open-loop commutation waveform is fed to the motor, lowering the wheel into the detent.

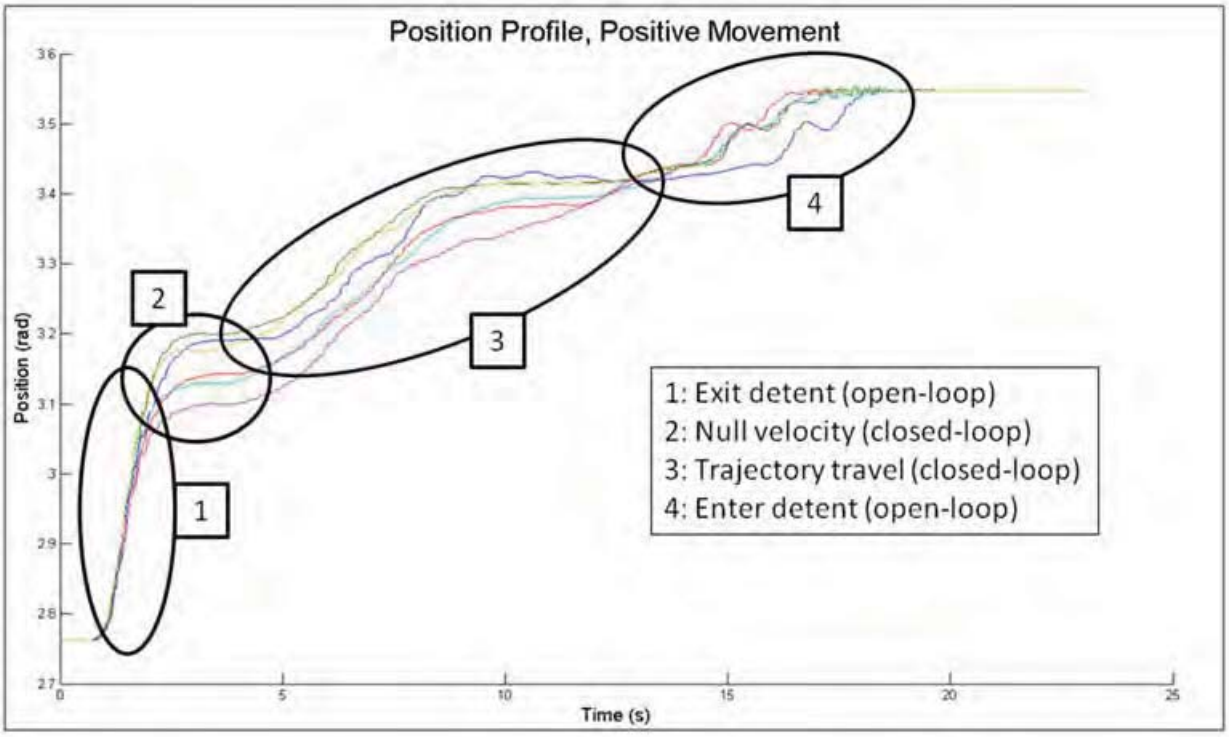

Figure 19. Pupil Select Mechanism Wheel Position Trajectories During Several Moves. Black Outlines Illustrate the Operation of the Multi-State Controller

Several types of fault detection and handling are built into the LabVIEW controller. The main purpose is to shut off the wheel if encoder data becomes unusable, but also watch for mechanical blockage of the wheel or unstable behavior. Every error condition sends a telemetry code and records data in the log file for analysis. Triggers include:

- **Encoder data rate.** If not enough packets are received in one time period, the connection is assumed to be set to the wrong frame rate or dropped completely, and the wheel is powered off.
- **Poor image decoding.** When the encoder CCD image cannot be parsed, the encoder system transmits an invalid code. If valid frames are received too infrequently, encoder calibration is the likely cause, and the wheel is powered off.

- **Trajectory tracking error.** If the wheel deviates too far from the command trajectory, it is assumed to be stuck or otherwise out of control, and the wheel is powered off.

The master ground system controls the PSM wheels with a special script that configures the encoder data transmission and performs error detection and automatic retries to move the wheel in a mostly autonomous fashion. This script was developed over the course of several years of use to properly handle edge cases such as powering up the system with the wheel in between two detents.

Infinite Microstepping Driver

The brushless motor was selected with a 60-V, 2.5-A peak winding configuration. This was to keep the current in the previously designed cryogenic harnesses within acceptable limits. However, it made most commercial motor drivers unusable, as they typically provide a maximum output around 28 V. When open-loop control was still intended, an “infinite microstepping” driver was designed for each motor using a pair of 16-bit Texas Instrument digital-to-analog converters and a pair of APEX high-power operational amplifiers configured as voltage-to-current amplifiers. The linear drives provide more stable fine control than pulse-width modulation drivers, and the current-mode output ensures that variations in harness and motor resistance over cryogenic temperatures does not affect the motor current/torque.

Each driver has a dsPIC microcontroller on board that can automatically produce high-fidelity sine/cosine commutation output or produce a desired phase angle and amplitude. The latter feature was used to achieve closed-loop control, where the LabVIEW program reads the encoder position and determines the optimal phase angle and amplitude required to produce the desired control torque. The drivers performed well in this application as well as their originally intended purpose—additional units were built to drive separate stepper motor mechanisms with extreme precision.

Assembly of the PSM, Functional and Performance Testing, and Integration into OSIM

The PSM was assembled at NASA Goddard Space Flight Center in Greenbelt, MD and initial performance testing of the PSM occurred in Spring 2011. The PSM was thermally cycled and taken to survival temperature limits with functional tests occurring at ambient temperature and pressure before testing, during the cold and hot operational limits, and again at ambient after thermal testing. During these functional tests, the PSM was able to show repeatable and stable element placement of less than 20 arc-seconds and was able to show compliance with all other functional and performance requirements. Figure 20 shows the PSM in the “Big Red” test dewar.

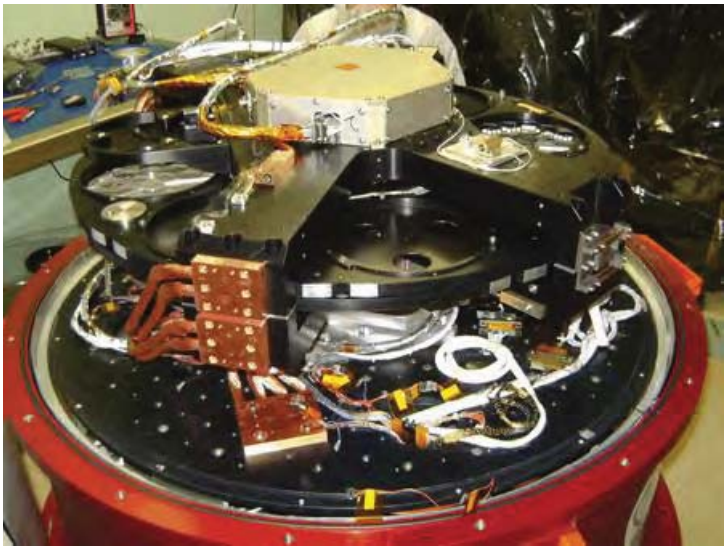

Figure 20. PSM During Initial Thermal Vacuum Performance Testing

To perform this testing, retroreflectors were used as alignment targets on the PSM X-Structure as a reference for cathetometer measurements taken of several fiducials and center markings engraved on the optical elements. The known machining error in the fiducial locations was then removed from the final data. For data collection, the wheels were rotated through the range of motion several times, approaching the detent position from different directions, stopping and powering off at each optical element location for measurement. Figure 21 shows the data collected for vacuum optical elements in the wheels.

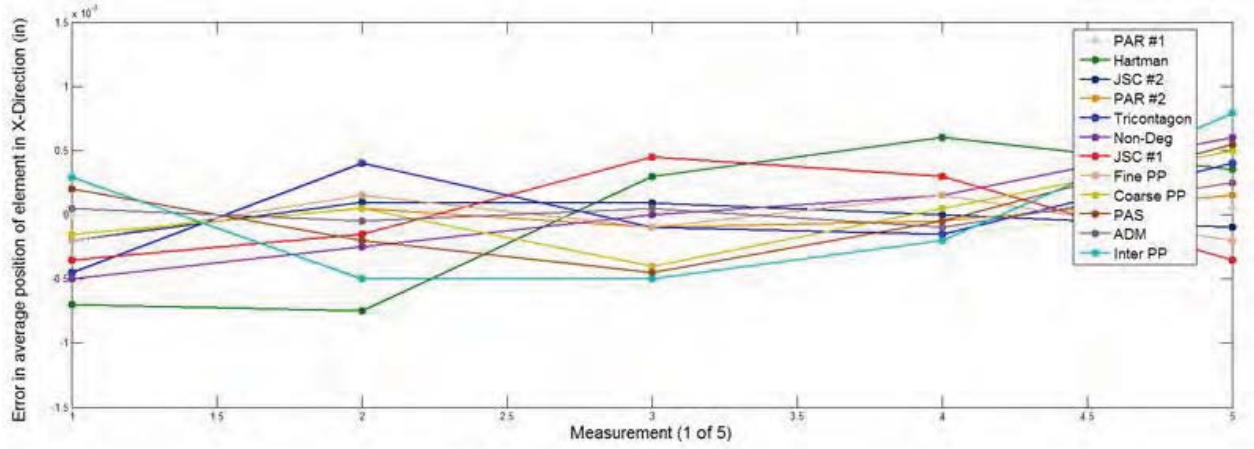

Figure 21. Error in the Repeatable Average Position (X-Direction) of Central Fiducial on Optical Elements

The PSM was integrated into OSIM with the other optical elements and mechanisms in the fall of 2011 in the Spacecraft Systems Development and Integration Facility (SSDIF) at GSFC. Figure 22 shows the PSM during integration in the SSDIF. With all of the components installed into OSIM, end-to-end ambient testing was performed and concluded in April 2012. The OSIM structure was then moved to the Space Environment Simulator (SES) chamber for calibration and verification of OSIM performance in a thermal vacuum environment. After 4½ months of testing at 100K, OSIM completed its first cryogenic vacuum test on August 2012. A second OSIM cryogenic test was performed at 100K on March 2013 and lasted 4 months. Figure 23 shows the PSM in the OSIM optical bench at the pupil plane between the two fold mirrors of the optical system.

Figure 22. PSM in SSDIF during assembly onto the OSIM bench

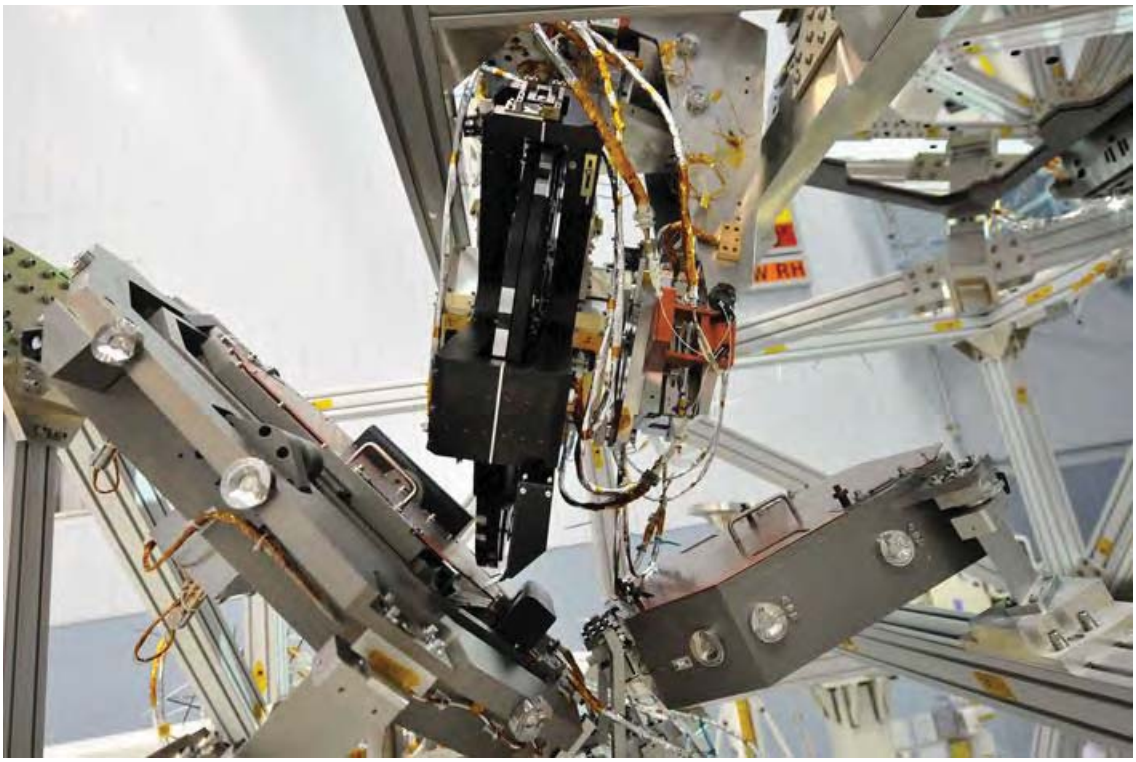

Figure 23. PSM as oriented in OSIM bench adjacent to fold mirror

Conclusion

The PSM is currently located in the SES chamber where it being used successfully in concert with other OSIM components for the test and calibration of the Integrated Science Instrument Module for JWST. The first three ISIM tests concluded in November 2013 with the next test projected to begin in May 2014. Due to project schedule constraints, the extreme cryogenic operating temperature of the mechanism, and the tight holding and repeatability requirements, several design features were incorporated into the PSM mechanism during different phases of the development. Included was the incorporation of a bearing and encoder system to survive the extreme operating temperature as well as the implementation of a challenging control system into the design late in the development. A special thank you to the entire OSIM team, especially the integration and test engineers as well as Dr. William Jones at Glenn Research Center for the use of facilities and expertise for friction characterization.

Lessons Learned

- Start early on proof-of-concept testing (especially those related to motor, bearing, and sensor selections) to flush out issues in the design with enough time to affect long lead purchases. Motors and encoder/sensor selection are key decision points in an electromechanical system design development and the suitability of these components should be revisited after any subsequent system level changes.
- Cold treated hybrid bearings consisting of Si_3N_4 balls, Cronidur 30 races, and a PGM-HT retainer have been shown to be suitable for cryogenic operations (down to 100K) in mechanisms with a low number of cycles.
- Though WearComp may be suitable for minimal debris in friction-based applications, care must be made that the mating surface is machined appropriately.

- When modeling a plant, ensure the plant is of a high enough fidelity to represent the dynamic response of the system accurately. When testing is used in conjunction with simulation, ensure the test item includes a realistic mass or inertia.
- Closed-loop control always needs a sensor with sufficient bandwidth and speed range. Sensor capabilities limit control possibilities, so selecting a good sensor is critical to anticipating future performance needs.
- In a two-pole system, where position is controlled via torque input, a first-order PID controller cannot track a quadratic position command (i.e. fixed acceleration curve) and it is better to use a higher-order transfer function as a compensator in these cases.
- Automatic event logging is critical in systems with many operators to capture intermittent issues. Producing clear and verbose log files from the very beginning of testing saves a lot of time detecting, diagnosing, and replicating bugs later on without having to re-run tests to duplicate anomalies.

References

Leviton, D.B. et al. "Cryogenic Optical Position Encoders for Mechanisms in the JWST Optical Telescope Element Simulator (OSIM)" *SPIE 8863* (2013)

Sullivan, J. et al. "Manufacturing and Integration Status of the JWST OSIM Optical Simulator" NTRS (2010)